Coherent State Transfer between an Electron and Nuclear Spin in $^{15}N@C_{60}$

Richard M. Brown,[1,*] Alexei M. Tyryshkin,[2] Kyriakos Porfyrakis,[1] Erik M. Gauger,[1] Brendon W. Lovett,[3,1] Arzhang Ardavan,[4] S. A. Lyon,[2] G. Andrew D. Briggs,[1] and John J. L. Morton[1,4]

[1]*Department of Materials, Oxford University, Oxford OX1 3PH, United Kingdom*
[2]*Department of Electrical Engineering, Princeton University, Princeton, New Jersey 08544, USA*
[3]*School of Engineering and Physical Sciences, Heriot Watt University, Edinburgh EH14 4AS, United Kingdom*
[4]*CAESR, Clarendon Laboratory, Department of Physics, Oxford University, Oxford OX1 3PU, United Kingdom*

(Received 23 November 2010; published 14 March 2011)

Electron spin qubits in molecular systems offer high reproducibility and the ability to self-assemble into larger architectures. However, interactions between neighboring qubits are "always on," and although the electron spin coherence times can be several hundred microseconds, these are still much shorter than typical times for nuclear spins. Here we implement an electron-nuclear hybrid scheme which uses coherent transfer between electron and nuclear spin degrees of freedom in order to both effectively turn on or off interqubit coupling mediated by dipolar interactions and benefit from the long nuclear spin decoherence times (T_{2n}). We transfer qubit states between the electron and ^{15}N nuclear spin in $^{15}N@C_{60}$ with a two-way process fidelity of 88%, using a series of tuned microwave and radio frequency pulses and measure a nuclear spin coherence lifetime of over 100 ms.

DOI: 10.1103/PhysRevLett.106.110504 PACS numbers: 03.67.Lx, 71.20.Tx, 76.30.−v, 81.05.ub

Hybrid quantum computing schemes aim to harness the benefits of multiple quantum degrees of freedom through the coherent transfer of quantum information between them. Such transfer has previously been shown between light and atomic ensembles [1,2], as well as electron to nuclear spin states in nitrogen vacancies [3] and ^{31}P donors [4], and progress is being made towards coupling electron spin ensembles to superconducting qubits [5,6]. Common motivations for state transfer between electron and nuclear spin qubits include the much longer decoherence times typically exhibited by the nuclear spin, and also the weaker dipolar interaction between nuclear spins, which allows interactions between neighboring qubits to be effectively turned off [3,4,7–11]. Both effects can be attributed to the relatively weak nuclear magnet moment, typically 3 orders of magnitude smaller than an electron spin. Thus, a powerful hybrid model for quantum computing is one where the electron spin qubit (which is more readily polarized and more quickly manipulated) is used for initialization and processing, while the nuclear spin is used as a memory. The presence of the electron spin also offers considerable advantages for the readout of a single qubit, either of the electron spin state directly [12,13] or a quantum nondemolition measurement of the nuclear spin [14,15].

Endohedral fullerenes (atoms held within a carbon cage) offer promise as molecular qubits due to their exceptionally long electron decoherence times [16–18] and convenient coupling to a local nuclear spin. This has led to various theoretical proposals that make use of both the electron and nuclear spin properties of these molecules [8–11,19]. Experimental examples of these include the use of $N@C_{60}$ to demonstrate polarization transfer from the electron to the nuclear spin and subsequent "bang-bang" decoupling [20], dynamic nuclear polarization [21], as well as generation of pseudoentanglement between the electron and nuclear spin [22,23]. The advantages of molecular spin qubits include the ability to use chemical methods to engineer precise electron dipolar interactions [24] and self-assembly into larger arrays [25,26]; however, this approach is limited by the "always-on" nature of dipolar interactions between neighboring spins. This is in contrast to systems such as donors in silicon, where precise qubit placement is more challenging, but where electrical gates could allow control of qubit interactions [7]. In this Letter we employ a molecular high spin system, comprising a ^{15}N atom encapsulated within a carbon cage: $^{15}N@C_{60}$. We select a spin concentration such that the electron dipolar coupling is of the order of $\sim$2 kHz. We transfer a coherent state from the electron to the nuclear spin degree of freedom, and show that this is able to effectively turn off the dipolar coupling between nearby qubits. We study the fidelity of the transfer process and investigate the decoherence time of the nitrogen nuclear spin at low spin concentrations.

The $^{15}N@C_{60}$ system consists of an $S = 3/2$ electron spin coupled via an isotropic hyperfine interaction of 22 MHz to the ^{15}N nuclear spin ($I = 1/2$). Under an applied magnetic field of $\sim 0.35T$, the energy level diagram is shown in Fig. 1(a), this produces a doublet in the electron spin resonance (ESR) spectrum where each line corresponds to a state of m_I [21]. To first order, the three electron $\Delta m_S = 1$ transitions in each m_I subspace have the same energy and cannot be addressed individually [27]. Thus a $\pi/2$ ESR pulse (selective on one m_I state) produces coherences across all three pairs of levels (with $\Delta m_S = 1$). For convenience, we will refer to an electron

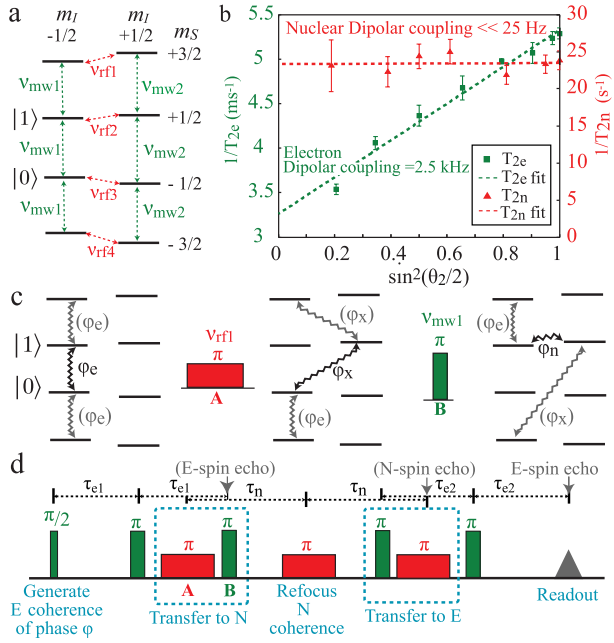

FIG. 1 (color online). (a) The coupled electron spin ($S = 3/2$), nuclear spin ($I = 1/2$) system for $^{15}N@C_{60}$ leads to 8 levels. A qubit can be represented across an electron spin transition where $m_I = -\frac{1}{2}$, $m_S = \pm\frac{1}{2}$ are denoted states $|0\rangle$ and $|1\rangle$. Transitions can be addressed via resonant microwave (mw) and radio frequency (rf) pulses. (b) Varying the length of the refocusing pulse θ_2 (see main text) allows a measure of the dipolar coupling between spin qubits, found to be much weaker when they reside in the nuclear spin than in the electron spin (data taken at 20 and 40 K, respectively). Because of the limited nuclear spin coherence time, only an upper bound for the nuclear dipolar coupling strength can be extracted. (c) Transfer of a qubit state from an electron spin degree of freedom to the ^{15}N nuclear spin, within the $m_S = +\frac{1}{2}$ subspace. Coherences are depicted by zigzag lines and "unwanted" coherences generated by the initial $\pi/2$ pulse on the $S = 3/2$ electron spin are shown in gray. At the end of the transfer sequence, such coherences will decay on the time scale of T_{2e} or faster, while the stored qubit will lose coherence on the time scale of T_{2n}. (d) The full two-way transfer sequence.

coherence between m_S levels $+\frac{1}{2}$: $-\frac{1}{2}$ as an *inner* coherence, and those between m_S levels $\pm\frac{3}{2}$: $\pm\frac{1}{2}$ as *outer* coherences. A qubit can be represented by the inner pair of m_S levels, in the subspace of $m_I = \frac{1}{2}$ [see Fig. 1(a)]. The T_{2e} we report here refers to this inner coherence [28].

We used dilute $^{15}N@C_{60}$ in a C_{60} matrix (2.5×10^{15} spins/cm^3), prepared by arc discharge and ion bombardment. The sample was purified using high performance liquid chromotography to remove unwanted amorphous material, placed in a quartz EPR tube, and pumped for several hours to remove paramagnetic O_2 before sealing. For pulsed EPR, we used an X band (9–10 GHz) Bruker Elexsys spectrometer and a low temperature helium-flow cryostat (Oxford CF935). Typical pulse lengths are 80 ns for a microwave (mw) π pulse using a traveling wave tube amplifier and 10 μs for a rf π pulse using a 500 W Amplifier Research solid-state amplifier.

The effect of the dipolar interaction between the electron spins of $^{15}N@C_{60}$ can be observed through a standard Hahn echo experiment ($\pi/2$-τ-θ_2-τ-echo) used to measure the electron spin decoherence time (T_{2e}) [29]. In this experiment the θ_2 pulse (which is typically π) acts to refocus effects such as magnetic field inhomogeneity as well as other interactions experienced by the spin which are constant on the time scale of τ. However, if the θ_2 pulse flips both the spin that is observed and a dipolar-coupled neighboring spin, the effect of this interaction is not refocused and the effective T_{2e} is reduced (this effect is termed instantaneous diffusion). If the θ_2 pulse is shortened it will act to refocus only a subset of spins and mimic a homogeneously dilute spin sample [29–31]. Plotting $1/T_{2e}$ vs $\sin^2(\theta_2/2)$, T_{2e} can then be extended from 190 μs using the standard Hahn echo sequence to an extrapolated 300 μs in the limit $\theta_2 = 0$ [see Fig. 1(b) and [28]]. From this measurement we extract a dipolar coupling of 2.5 kHz between electron spins at the average $N@C_{60}$ separation [28], which we will show is not present between nuclear spins.

To probe the nuclear spin qubit we employ the transfer sequence shown in Fig. 1 to propagate an electron coherence to a nuclear coherence. The implementation of this sequence is complicated compared to previous studies [4] by the presence of the $S = 3/2$ electron spin, such that the initial $\pi/2$ mw pulse produces both an inner coherence and unwanted outer coherences. The application of a rf π pulse on the $m_S = +\frac{1}{2}$ transition (a controlled-NOT in quantum gate terminology) transfers the qubit to an electron-nuclear cross coherence (φ_x). A mw π pulse selective on $m_I = -\frac{1}{2}$ then completes the SWAP operation to produce a nuclear coherence (φ_n). Unwanted outer coherences generated during the sequence remain as both electron- and multiple-quantum coherences, which decay on the time scale of the electron spin decoherence time (T_{2e}) or faster [28]. The desired nuclear spin coherence can then be stored for many milliseconds before transfer back to the electron spin via a reverse of the sequence and readout by a conventional electron spin (Hahn) echo. The full sequence is shown in Fig. 1 with the addition of carefully placed pulses to refocus the effect of inhomogeneous broadening on the spin packets in electron, nuclear, and multiple quantum coherences. It is not possible to store the qubit within a nuclear coherence in the $m_S = \pm\frac{3}{2}$ subspaces using this sequence, but they are considered in the supplementary material [28].

There are a number of ways to confirm that the recovered electron spin echo arises solely from a state which was stored in a nuclear spin degree of freedom. One method is to apply a time-varying phase shift to the nuclear spin (e.g., a geometric phase gate [32]) and observe a corresponding phase shift in the electron spin echo. This measurement shows no evidence of any other contribution to the electron

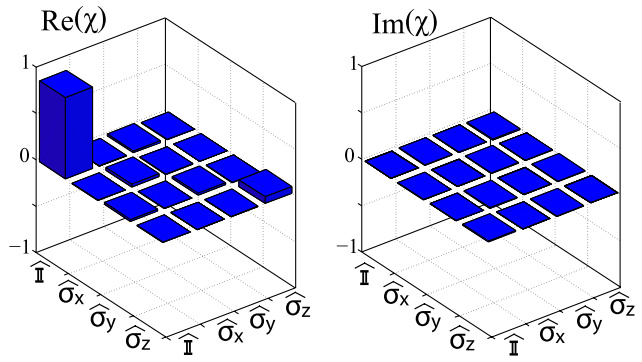

FIG. 2 (color online). Quantum process tomography matrix (χ) for the transfer of a qubit state from the electron to the nuclear degree of freedom and back, in the basis ($\mathbb{1}$, σ_x, σ_y, σ_z). χ is evaluated given reference and recovered matrices and gives a fidelity compared to a perfect $\mathbb{1}$ of 0.88.

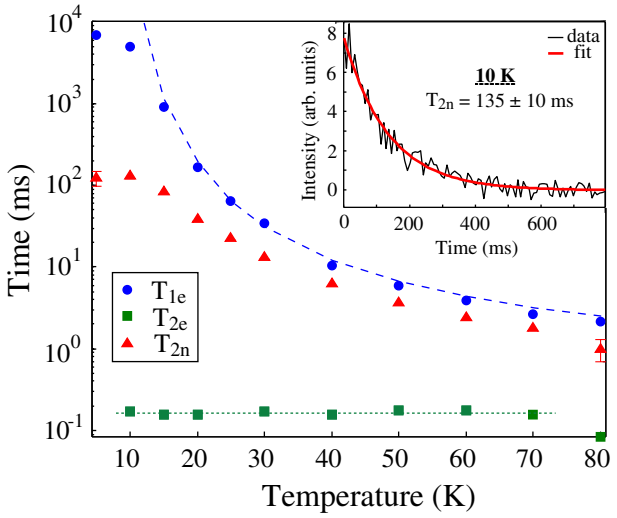

FIG. 3 (color online). Relaxation and decoherence times as a function of temperature: T_{1e} (blue, circle), T_{2e} (green, square), T_{2n} (red, triangle), from monoexponential fits with error less than the marker size unless shown. The dashed line is a fit to an Arrhenius temperature dependence for T_{1e}. The dotted line for T_{2e} is a guide. Inset: The nuclear decoherence curve with a monoexponential fit to 135 ± 10 ms at 10 K.

spin echo, and is described in more detail in the supplementary material [28]. Ultimately, the success of the transfer scheme is shown by the ability to recover any input state with high fidelity after storage in the nuclear spin. This is achieved by exciting the full electronic and nuclear transitions, made possible by the short pulse lengths used and the narrow intrinsic sample ESR and NMR linewidths $<$0.6 MHz and 15 kHz, respectively. We prepare the input states, $\pm X$, $\pm Y$, and $\pm Z$, by varying the phase of the initial $\pi/2$ mw pulse ($\pm X$, $\pm Y$), applying an initial π pulse ($+Z$), or by removing the initial pulse ($-Z$). Using quantum process tomography we can then extract the process matrix for the transfer scheme, χ, in the basis ($\mathbb{1}$, σ_x, σ_y, σ_z) [33]. To accurately evaluate χ we compare the recovered states from the transfer sequence with those given by an ordinary Hahn echo ($\tau = \tau_{e1} + \tau_{e2}$). Thus, χ incorporates any losses at the storage or retrieval step, as well as during the storage period in the nuclear spin, but not any errors associated with the state generation or measurement. Figure 2 shows the measured χ, giving a fidelity of 0.88, compared to the ideal identity process ($\mathbb{1}$). We attribute this fidelity primarily due to errors in the transfer pulses—the use of BB1 composite mw pulses improves the fidelity for the $+X$ state from 90% to 94% and we would expect further improvement with composite rf pulses (see supplementary material [28]).

The nuclear decoherence time (T_{2n}) can be found by varying the time the qubit is held within the nuclear spin state ($2\tau_n$). The resulting exponential decay in echo intensity gives T_{2n} as long as 135 ± 10 ms (at 10 K). At this temperature, T_{2e} is 160 μs, and thus the nuclear memory gives almost 3 orders of magnitude improvement in the decoherence time. Nuclear dipolar coupling can be assessed through the effect on T_{2n} of an "instantaneous diffusion" experiment, similar to that applied on the electron spin. Reducing the length of the nuclear refocusing pulse [$0.2 \leq \sin^2(\theta_{\rm rf}/2) \leq 1.0$, see Fig. 1(b)] results in no appreciable change in T_{2n} at 20 K. Hence, coherent transfer reduces the interqubit coupling term from the electron-electron dipolar constant to the nuclear-nuclear dipolar interaction which we show to be weak as expected, $\ll$ 25 Hz [34].

The temperature dependence of the fundamental spin relaxation parameters in the system are shown in Fig. 3. The electron relaxation time T_{1e} [measured by a standard inversion recovery sequence, π-τ-$\pi/2$-T-π-T-echo [29]] is shown to increase exponentially with decreasing temperature. This follows an Arrhenius dependence, consistent with a two-phonon process resonant with an excited vibrational mode [17,35] and can reach several seconds at low temperatures. Electron spin flips (whose time scale is characterized by T_{1e}) ultimately act to limit the nuclear coherence time. In the temperature range, 50–80 K, we find that T_{2n} follows T_{1e} with the experimentally determined relationship $T_{2n} \sim 0.6T_{1e}$. Below 50 K, a secondary mechanism is evident that limits the nuclear decoherence time to ~130 ms. We analytically model relaxation in the system by applying the Lindblad equation, with the relevant raising and lowering operators, to a given initial state (e.g., a pure nuclear coherence, for T_{2n} or inverted electron state, for T_{1e}):

$$\dot{\rho} = -\gamma_a(\rho S^{\mp}S^{\pm} + S^{\mp}S^{\pm}\rho - 2S^{\pm}\rho S^{\mp}) - i[\mathcal{H}, \rho], \quad (1)$$

where γ_a represents both γ_1, the electron spin relaxation rate between the m_S levels $\pm\frac{3}{2} \leftrightarrow \pm\frac{1}{2}$, and γ_2, the relaxation rate between m_S levels $\frac{1}{2} \leftrightarrow -\frac{1}{2}$. The raising and lowering operators are given by S^+ and S^-. Applying relaxation in the high temperature limit and assuming no direct nuclear relaxation, the relevant density matrix elements show a nuclear dephasing rate, $\Gamma_n = (3\gamma_1 + 4\gamma_2)$. Similarly, taking Eq. (1) and solving a series

of coupled linear equations the electron polarization is expressed in terms of two parts:

$$P(t) = \alpha e^{-\lambda_- t} + \beta e^{-\lambda_+ t}, \quad (2)$$

where α and β are prefactors which are a function of γ_1 and γ_2, and the eigenvalues λ are given by

$$\lambda_\pm = \Gamma_n \pm \sqrt{(3\gamma_1)^2 + (4\gamma_2)^2}. \quad (3)$$

It can be shown that the slower decaying component, λ_-, must be dominant, which gives a maximum ratio of $\lambda_- = \Gamma_e \sim 0.3\Gamma_n$ ($T_{2n} \sim 0.3T_{1e}$), when $3\gamma_1 = 4\gamma_2$. To reconcile this ratio with the experimentally obtained $T_{2n} \sim 0.6T_{1e}$, additional relaxation processes can be included in the model; for instance, if γ_3 is given by $m_S = \pm\frac{3}{2} \leftrightarrow m_S = \mp\frac{1}{2}$, then when $\gamma_1 = \gamma_3 \geq \gamma_2$ a theoretical T_{2n} of up to $2/3T_{1e}$ can be found.

In conclusion, we have reported the coherent transfer of qubit states between electron and nuclear spin degrees of freedom, in a high spin system. The quantum process tomography of the two-way transfer shows a fidelity of 88%, while we measure a nuclear decoherence time of up to 130 ms, almost 3 orders of magnitude longer than the electron spin coherence time. Thus, the ^{15}N nuclear spin can be employed as both a quantum memory and to effectively turn off interqubit coupling. This is a crucial element in the realization of fullerene hybrid quantum computing schemes that exploit the nuclear and electron spin [8–11,19], especially given recent work in producing larger fullerene architectures [24]. Alternatively, the coupling between spin ensembles and cavities could be exploited [5,6], along with the storage of multiple microwave excitations [36], to produce a robust multimode nuclear memory.

We thank Stephanie Simmons for helpful discussions and instrumentation support. The research is supported by the NSF through the Princeton MRSEC under Grant No. DMR-0213706 and the EPRSC through IMPRESS (EP/D074398/1), and CAESR (EP/D048559/1). J. J. L. M., B. W. L., and A. A. are supported by the Royal Society.

*richard.brown@materials.ox.ac.uk

[1] B. Julsgaard *et al.*, Nature (London) **432**, 482 (2004).
[2] T. Chanelière *et al.*, Nature (London) **438**, 833 (2005).
[3] M. V. G. Dutt *et al.*, Science **316**, 1312 (2007).
[4] J. J. L. Morton *et al.*, Nature (London) **455**, 1085 (2008).
[5] D. I. Schuster *et al.*, Phys. Rev. Lett. **105**, 140501 (2010).
[6] Y. Kubo *et al.*, Phys. Rev. Lett. **105**, 140502 (2010).
[7] B. E. Kane, Nature (London) **393**, 133 (1998).
[8] C. Ju, D. Suter, and J. Du, Phys. Rev. A **75**, 012318 (2007).
[9] W. L. Yang *et al.*, Phys. Rev. A **81**, 032303 (2010).
[10] D. Suter and K. Lim, Phys. Rev. A **65**, 052309 (2002).
[11] W. Harneit *et al.*, Phys. Status Solidi B **233**, 453 (2002).
[12] A. Morello *et al.*, Nature (London) **467**, 687 (2010).
[13] F. Jelezko *et al.*, Phys. Rev. Lett. **92**, 76401 (2004).
[14] M. Sarovar *et al.*, Phys. Rev. B **78**, 245302 (2008).
[15] P. Neumann *et al.*, Science **329**, 542 (2010).
[16] R. M. Brown *et al.*, Phys. Rev. B **82**, 033410 (2010).
[17] J. J. L. Morton *et al.*, J. Chem. Phys. **124**, 014508 (2006).
[18] W. Harneit, Phys. Rev. A **65**, 032322 (2002).
[19] S. C. Benjamin *et al.*, J. Phys. Condens. Matter **18**, S867 (2006).
[20] J. J. L. Morton *et al.*, Nature Phys. **2**, 40 (2005).
[21] G. W. Morley *et al.*, Phys. Rev. Lett. **98**, 220501 (2007).
[22] M. Mehring, W. Scherer, and A. Weidinger, Phys. Rev. Lett. **93**, 206603 (2004).
[23] B. Naydenov *et al.*, Phys. Status Solidi B **245**, 2002 (2008), .
[24] G. Gil-Ramírez *et al.*, Org. Lett. **12**, 3544 (2010).
[25] A. N. Khlobystov *et al.*, J. Mater. Chem. **14**, 2852 (2004).
[26] A. N. Khlobystov, D. A. Britz, and G. A. D. Briggs, Acc. Chem. Res. **38**, 901 (2005).
[27] J. J. L. Morton *et al.*, J. Chem. Phys. **122**, 174504 (2005).
[28] See supplemental material at http://link.aps.org/supplemental/10.1103/PhysRevLett.106.110504 for details including outer coherence and fidelity measurements.
[29] A. Schweiger and G. Jeschke, *Principles of Pulse Electron Paramagnetic Resonance* (Oxford University Press, Oxford, England, 2001);
[30] J. R. Klauder and P. W. Anderson, Phys. Rev. **125**, 912 (1962).
[31] A. M. Tyryshkin *et al.*, Phys. Rev. B **68**, 193207 (2003).
[32] S. Simmons *et al.*, Nature (London) **470**, 69 (2011).
[33] M. A. Nielsen and I. L. Chuang, *Quantum Computation and Quantum Information* (Cambridge University Press, Cambridge, England, 2000), p. 389.
[34] We extract only an estimated upper bound for the nuclear-nuclear dipolar coupling due to the limit of T_{2n}. The dipolar coupling is expected to be $\sim 10^6$ weaker between nuclear spins compared to electron spins and thus of order mHz.
[35] J. J. L. Morton *et al.*, Phys. Rev. B **76**, 085418 (2007).
[36] H. Wu *et al.*, Phys. Rev. Lett. **105**, 140503 (2010).